Anode-Driven In Situ-Formed Electrolytes Enable Rechargeable Calcium Metal Batteries

ACS MATERIALS LETTERS

www.acsmaterialsletters.org
Letter

Anode-Driven *In Situ*-Formed Electrolytes Enable Rechargeable Calcium Metal Batteries

Zaher Slim,* Hanna Andersson, and Patrik Johansson

Cite This: *ACS Materials Lett.* 2026, 8, 1761−1767

ABSTRACT: Calcium's high reactivity typically causes surface passivation, limiting its applicability in electrochemical devices, such as batteries. Here we harness this very reactivity to generate an electrolyte both *ex situ* and, most importantly, *in situ*, by reacting Ca metal with a Ca-free precursor solution comprising tris(2,2,2-trifluoroethyl) borate ($B(Otfe)_3$; Otfe = OCH_2CF_3) and 2-methoxyethylamine (MOEA) in 1,2-dimethoxyethane (DME). The resulting electrolyte enables reversible Ca electrochemistry in symmetric, half-, and full cells, including at −10 °C. By combining electrochemistry with FTIR spectroscopy, XPS, and DFT calculations, we are able to propose a synergistic mechanism in which $B(Otfe)_3$ reacts at the Ca metal surface to form anionic borate species and a Ca^{2+}-conducting interphase, while the Ca^{2+} released from the anode is stabilized in the solution/electrolyte by MOEA coordination. This metal-driven, interfacial strategy provides an alternative to the salt-in-solvent paradigm for electrolyte preparation and suggests a broadly applicable route for electrolyte generation directly from reactive-metal anodes.

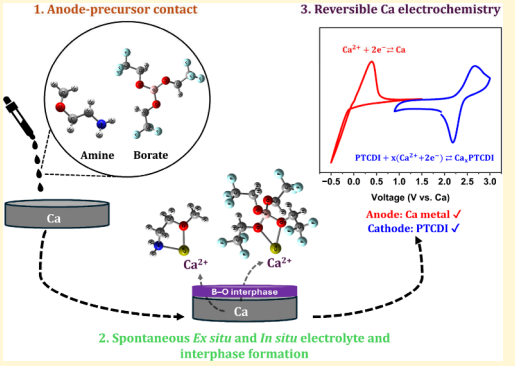

Calcium (Ca) metal plating/stripping has gained increasing attention not only for calcium metal batteries (CMBs),[1] but also for emerging applications targeting diverse goals, such as electrochemical ammonia synthesis and recovery of rare-earth elements.[2,3] While encouraging progress has been made, this challenging process remains limited in success to a small number of electrolytes.[1,4−11] Many of these rely on finely tuned Ca^{2+} solvation and on Ca-salts that are moisture-sensitive, costly, and quite often require complex synthesis—factors that, both individually and collectively, pose practical barriers for deployment.

Thus far, reported CMB electrolytes have primarily relied on a salt-in-solvent approach, in which a Ca-salt is dissolved in a solvent prior to cell assembly. Reversible Ca metal electrochemistry has been demonstrated across several electrolyte families, including borate- and aluminate-based salts, hydridoborate and halide chemistries (*e.g.*, CaI_2), and strongly solvating solvent(s).[4−8,10−13] However, these electrolyte families face persistent trade-offs, such as multistep syntheses, water contamination, limited anodic stability, solvent decomposition, or limited salt solubility.[13] As a result, CMB electrolyte development remains at an exploratory R&D stage and the practical future of CMBs is still uncertain, underscoring the need to further expand the electrolyte design space.

At the core of these limitations lies calcium's inherent reactivity at the electrode/electrolyte interface, which drives formation of passivating interphases that ultimately terminate the electrochemistry. Mechanistic studies have shown that the composition and structure of the passivation layer are key to reversible Ca plating/stripping.[14] Accordingly, additive-driven SEI engineering, including boron-based functional additives, has emerged as an effective approach to enable Ca electrochemistry.[11,15,16]

More generally, this passivation challenge is not unique to Ca; Mg metal anodes exhibit similar reactivity, and Song et al.[17] recently introduced an *in situ* electrolyte-formation strategy via spontaneous reaction at the Mg metal surface during cell assembly. Similarly, we recently showed that Ca metal anodes, under appropriate solvation conditions, can sustain stable cycling in symmetric Ca||Ca cells without predissolved Ca salts,[13] suggesting *in situ* generation of Ca^{2+}-containing charge carriers and, consequently, electrolyte formation driven by calcium's surface reactivity.

Building on these insights, we designed a Ca-free precursor solution that leverages Ca-metal interfacial chemistry to generate an electrolyte directly from Ca metal upon contact, either during coin cell assembly (*in situ*) or outside the cell (*ex situ*) by soaking the Ca-foil in the precursor solution. The precursor comprises tris(2,2,2-trifluoroethyl)borate (B-

Received: March 16, 2026
Revised: April 12, 2026
Accepted: April 17, 2026
Published: April 21, 2026

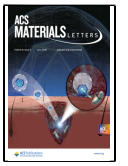

https://doi.org/10.1021/acsmaterialslett.6c00259
ACS Materials Lett. 2026, 8, 1761−1767

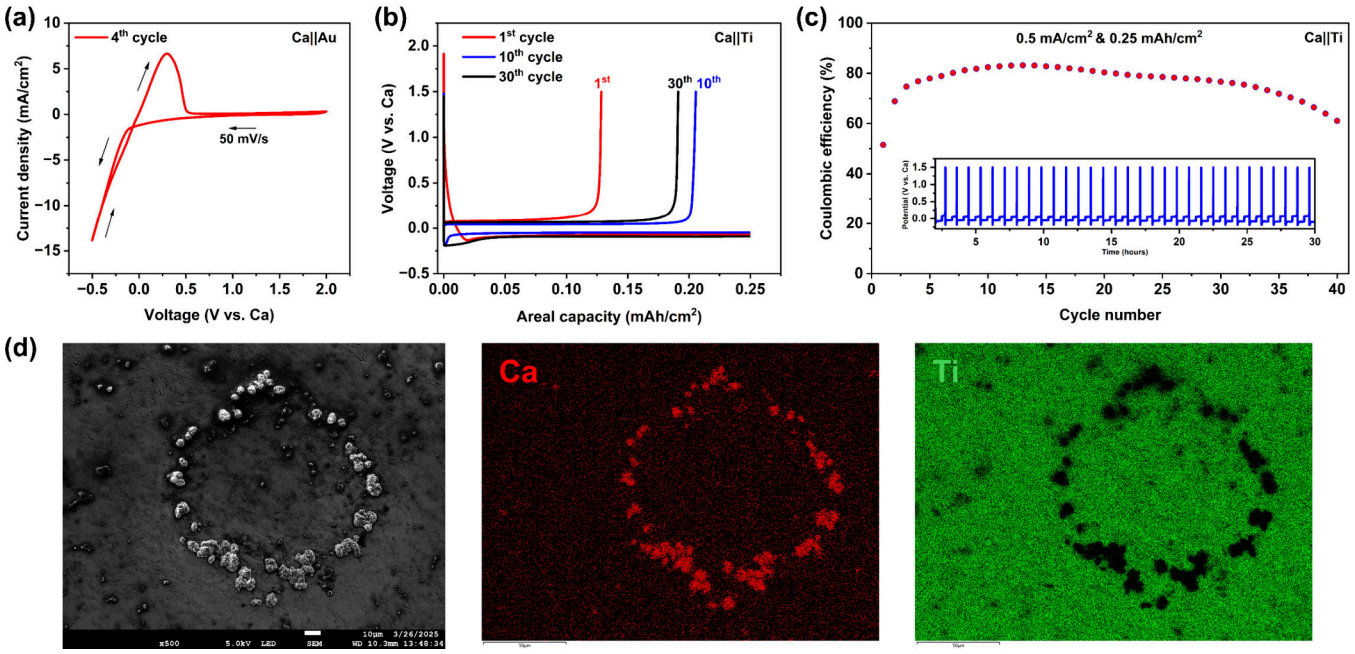

Figure 1. Electrochemical performance and characterization of Ca half-cells using the $B(Otfe)_3$ + MOEA in DME precursor. (a) CV of a Ca||Au coin cell. (b) Selected charge−discharge cycles of Ca||Ti coin cells at 0.5 mA/cm^2. (c) Corresponding coulombic efficiency of panel b, with the inset showing voltage−time profiles. (d) SEM image and EDX elemental map of Ca deposited on Ti at 0.1 mA/cm^2 for 4 h.

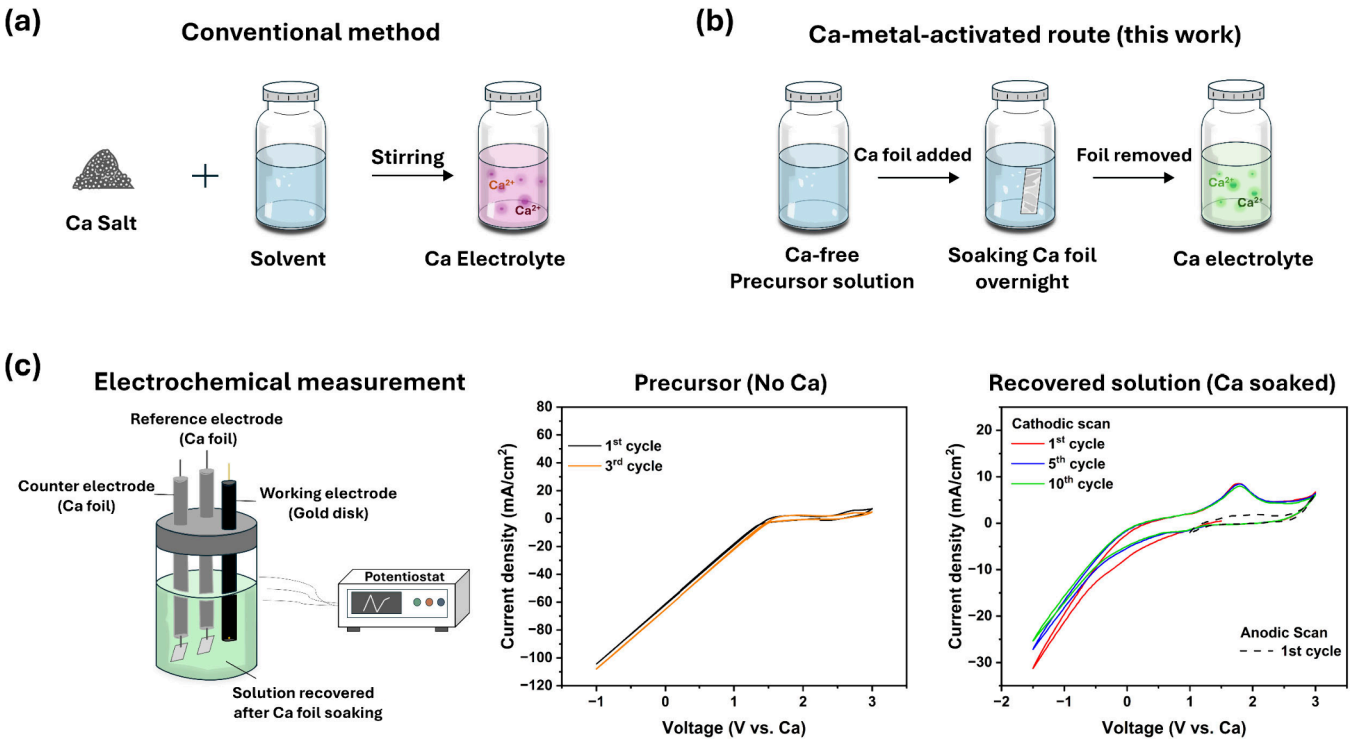

Figure 2. Comparison of electrolyte preparation routes and beaker-cell validation. (a) Conventional method. (b) Ca-metal-activated route (this work). (c) Beaker-cell configuration and representative CVs at 50 mV/s showing that the precursor solution is largely inactive, whereas the Ca-soaked (recovered) solution/electrolyte exhibits redox activity at a Au working electrode.

$(Otfe)_3$;Otfe = OCH_2CF_3) and 2-methoxyethylamine (MOEA) in 1,2-dimethoxyethane (DME). $B(Otfe)_3$ has previously shown promise in supporting Ca plating/stripping;[11] here it is used as a borate-based reactive component expected to contribute to electrolyte and interphase formation, while MOEA is introduced to enhance the kinetics by optimizing the Ca^{2+} solvation.[18] To this end, we combine electrochemistry, spectroscopies, and density functional theory (DFT) calculations to connect electrolyte behavior with solution speciation, interphase composition, and finally reversible Ca electrochemistry.

To correlate electrochemical performance with electrolyte chemistry, we first evaluate the *in situ*−formed electrolyte in Ca||Au and Ca||Ti coin cells and corroborate Ca deposition

https://doi.org/10.1021/acsmaterialslett.6c00259
ACS Materials Lett. 2026, 8, 1761−1767

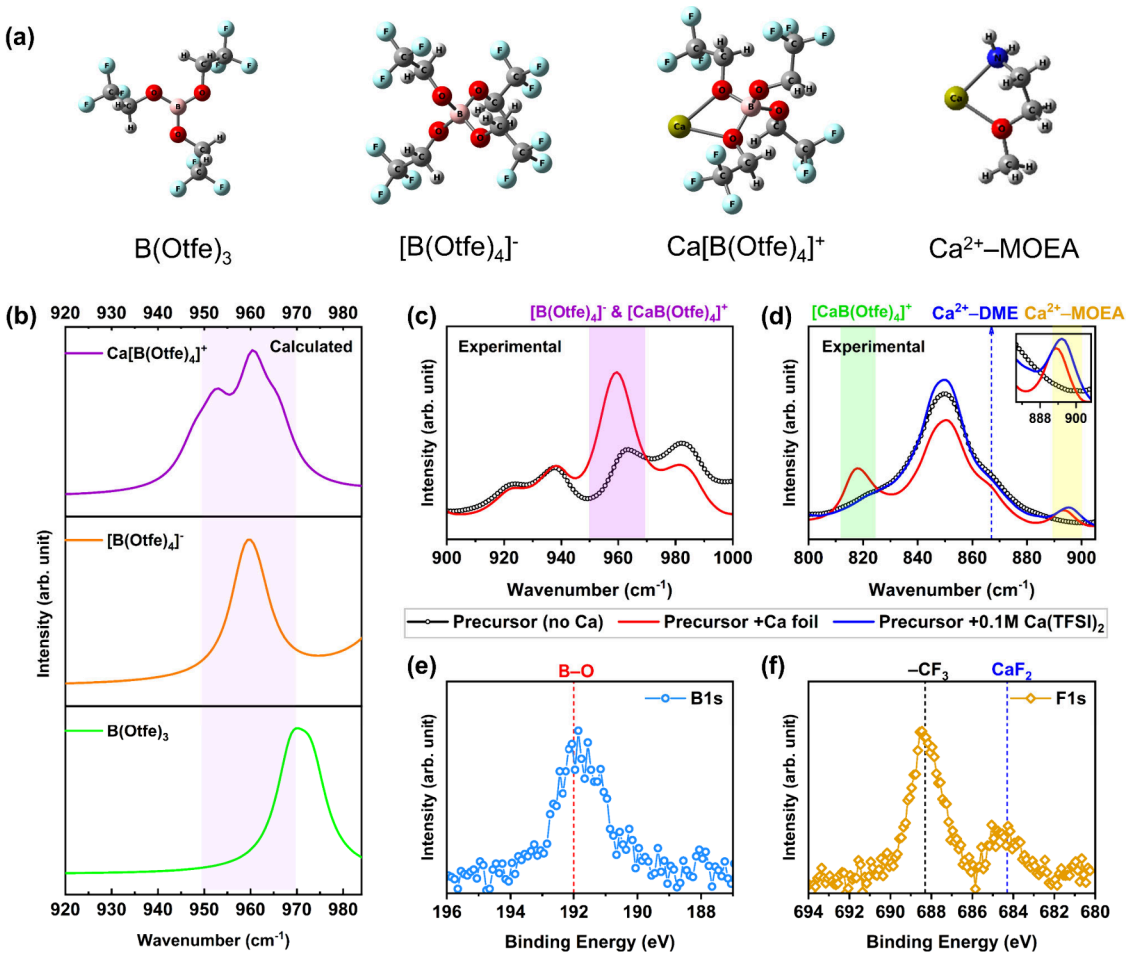

Figure 3. (a) DFT-optimized structures of borate, Ca^{2+}–borate, and Ca^{2+}–MOEA species. (b) DFT-calculated artificial FTIR spectra in the CH_2 rocking region for borate and Ca^{2+}–borate species. (c, d) Selected FTIR spectra regions of the precursor solution before and after Ca contact, compared with a conventional electrolyte (0.1 M $Ca(TFSI)_2$ in precursor solution). (e, f) Raw B 1s and F 1s XPS spectra of Ca foil after soaking in the precursor solution.

using SEM/EDX. We then probe precursor-to-electrolyte conversion and interphase formation via FTIR spectroscopy (with the analysis supported by DFT calculations) and XPS. Finally, we evaluate cycling stability in Ca||Ca symmetric and Ca||PTCDI (perylene-3,4,9,10-tetracarboxylic acid diimide) full-cell configurations to assess the *in situ*–formed electrolyte for CMBs. Additional experimental details are provided in the Supporting Information (SI).

We began by investigating Ca metal electrochemistry in $B(Otfe)_3$ in DME and separately in MOEA in DME in order to better understand the contributions of each component individually. Cyclic voltammetry (CV) using Ca||Au coin cells revealed no indications of Ca plating or stripping (Figure S1), indicating that neither component alone is sufficient. When $B(Otfe)_3$ and MOEA were combined in a 1:2 (v/v) ratio (see Design Rationale in the SI), however, the CV revealed characteristic signatures of reversible plating/stripping (Figure 1a). To further evaluate this electrochemical behavior and assess its reproducibility on alternative substrates, we performed CV (Figure S 1d) and galvanostatic cycling (GC) using titanium (Ti) electrodes (Figure 1b). The GC of Ca||Ti cells showed stable plating/stripping at 0.5 mA/cm^2 with a capacity of 0.25 mAh/cm^2, maintaining performance for 40 cycles with a coulombic efficiency (CE) reaching up to 80% (Figure 1c). Notably, even at a higher current density (1 mA/cm^2) and lower areal capacity (0.05 mAh/cm^2), the cells cycled stably for 200 cycles, with over 85% CE (Figure S2a). Hence, the synergistic interaction between $B(Otfe)_3$ and MOEA enables stable and reversible Ca plating/stripping, remarkably without the addition of any Ca-salt to the solution.

To confirm that the observed electrochemical activity corresponds to actual Ca plating, we performed SEM analysis after constant-current plating on a Ti substrate. A ring-shaped pattern of deposits was observed and identified as Ca via EDX mapping (Figure 1d). Similar morphologies were also found on Au substrates (Figure S3), supporting Ca plating on different substrates.

We next assessed electrolyte formation *ex situ* by soaking a Ca metal foil in the precursor solution and recovering the resulting solution/electrolyte (Figure 2). This serves two purposes: (i) it enables controlled exposure of the Ca foil and evaluation of the emergent electrolyte in a conventional three-electrode beaker cell (Figure 2c), and (ii) it provides samples for electrolyte-structure analysis via FTIR spectroscopy (Figure 3). The recovered solution/electrolyte was first evaluated in the three-electrode beaker-cell configuration (Figure 2c) and compared with the CV response of the precursor solution (control). While the beaker-cell CV differs in some features from the coin-cell response (Figure 1a), the recovered solution/electrolyte exhibits reversible redox behavior con-

https://doi.org/10.1021/acsmaterialslett.6c00259
ACS Materials Lett. 2026, 8, 1761−1767

Scheme 1. Ca-Metal-Driven Electrolyte Formation and Operation[a]

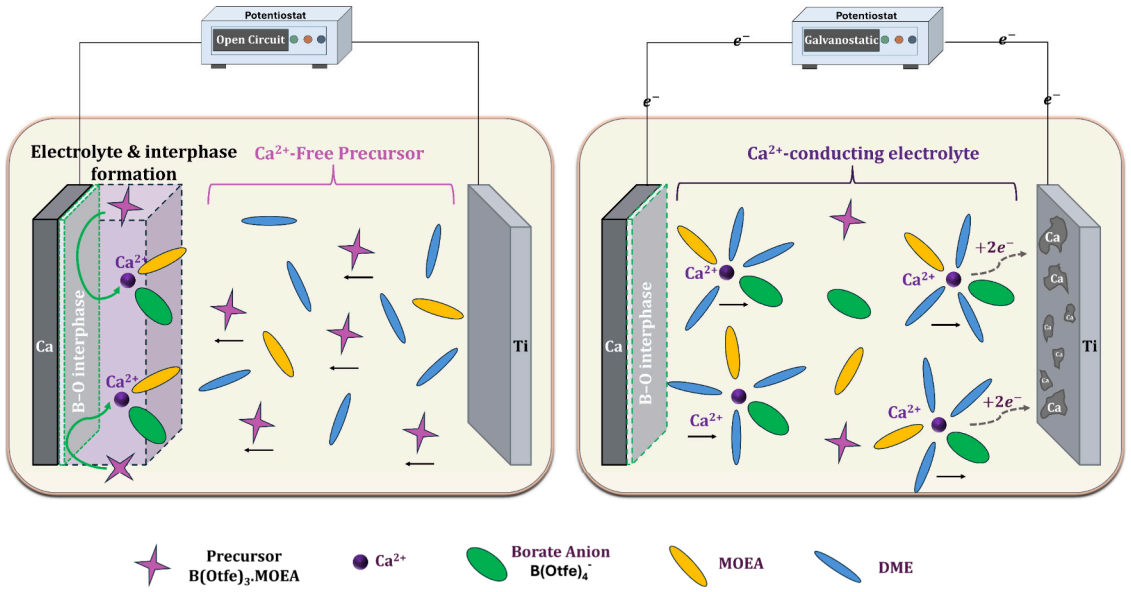

[a]Left: At OCV, the precursor solution reacts at the Ca metal anode to generate a Ca^{2+}-conducting electrolyte and a B−O-based interphase. Right: Under galvanostatic conditions, the *in situ* formed electrolyte enables Ca plating on Ti.

sistent with Ca plating/stripping, in line with prior reports on related aluminate-based electrolytes.[9] In contrast, the precursor solution shows only continuous reductive decomposition with no corresponding redox features. Analogous experiments with Mg are shown in Figure S4.

With reversible electrochemical activity established both *in situ* and *ex situ*, we next elucidate how the precursor solution reacts with Ca metal by combining FTIR spectroscopy with DFT-calculated vibrational spectra to first determine the solution speciation. In parallel, XPS was used to characterize the resulting interphase composition.

Our first working hypothesis was that $B(Otfe)_3$ is converted upon contact with Ca metal into a tetrakis(2,2,2-trifluoroethoxy)borate anion, $[B(Otfe)_4]^-$, which then can form Ca-borate contact ion pairs (CIPs), $[Ca{-}(B(Otfe)_4)]^+$. This hypothesis is supported by Mg-electrolyte literature showing that $B(Otfe)_3$ can be converted to $[B(Otfe)_4]^-$ via *in situ* (one-pot) synthesis.[19,20] Using experimental FTIR spectra, DFT-optimized structures and corresponding artificial spectra (Figure 3a−d, Table S1, Figure S5) we first found computationally that the characteristic CH_2 rocking band for $B(Otfe)_3$ at 970 cm^{-1} is shifted to 960 cm^{-1} for $[B(Otfe)_4]^-$ and for $[Ca(B(Otfe)_4)]^+$ the artificial spectrum exhibits two broadened features at 952 and 960 cm^{-1} with a shoulder near 965 cm^{-1}, indicating multiple, perturbed CH_2 environments upon Ca^{2+}−anion ion pairing (Figure 3b).

Experimentally, the $B(Otfe)_3$ + MOEA in DME spectrum shows a band at ∼963 cm^{-1}, which upon contact with Ca evolves into a broad, high-intensity envelope centered near 960 cm^{-1} and spanning ∼950−975 cm^{-1}, suggesting formation of both $[B(Otfe)_4]^-$ and $[Ca{-}(B(Otfe)_4)]^+$ CIPs (Figure 3c).

There are additional bands in the 800−910 cm^{-1} region that emerge after Ca contact; the distinct peak at 820 cm^{-1} is assigned to an asymmetric B−O stretching + symmetric C−C−F bending mode vibration of $[Ca(B(Otfe)_4)]^+$ (calcd. 824 cm^{-1}) while the peak at 893 cm^{-1} is assigned to Ca^{2+}−MOEA coordination (calcd. 882 cm^{-1}), whereas the weak shoulder near 865 cm^{-1} likely includes a Ca^{2+}−DME coordination contribution. The above assignments are further supported by FTIR spectra of conventional "salt-in-solvent" electrolytes, whereas 0.3 M $Ca(TFSI)_2$ in DME exhibits a band at 867 cm^{-1} (Figure S6b) and 0.3 M $Ca(TFSI)_2$ in neat MOEA shows a corresponding band at 895 cm^{-1} (Figure S6a).

We stress that no such spectral changes were observed when Ca metal was contacted separately with $B(Otfe)_3$, MOEA, or DME; they emerged only for the precursor solution, and as this aligns with the observation of reversible Ca plating/stripping, this indicates that the combined $B(Otfe)_3$−MOEA formulation stabilizes Ca^{2+} in solution and enables reversible Ca electrochemistry.

In addition, the ν(N−H) mode region provides evidence for Ca^{2+}−MOEA coordination; the band shifts from 3380 cm^{-1} in MOEA to ∼3430 cm^{-1} (Figure S5). Similar ν(N−H) shifts have been reported for amide-based electrolytes[21] and are also supported by our DFT calculations.

Overall, these observations support that $B(Otfe)_3$ decomposes at the Ca metal surface to form borate species, while MOEA stabilizes Ca^{2+} in solution, thereby forming an electrolyte that enables reversible Ca plating/stripping (Scheme 1). DME acts primarily as a diluent, moderating the reactivity of Ca and suppressing excessive decomposition; without DME, the precursor exhibited unusually high cathodic current densities, consistent with severe reductive decomposition, although plating/stripping-like features were initially observed in the CV (Figure S7a).

To probe interphase chemistry during static conditioning, Ca‖Ti coin cells were assembled and rested at open circuit voltage (OCV) for 2 h before disassembly, and X-ray photoelectron spectroscopy (XPS) was performed on the retrieved Ca metal anodes. The resulting spectra reveal borate-derived and fluorine-containing surface species; the B 1s region (192−193 eV) is consistent with B−O/B−OR environments (Figure 3e), in agreement with literature,[14] and the F 1s envelope (Figure 3f) comprising a feature at 688−689 eV and another at ∼684.5 eV, is attributed to organic C−F (e.g., $-CF_3$) from Otfe-derived fragments and/or residual borate

https://doi.org/10.1021/acsmaterialslett.6c00259
ACS Materials Lett. 2026, 8, 1761−1767

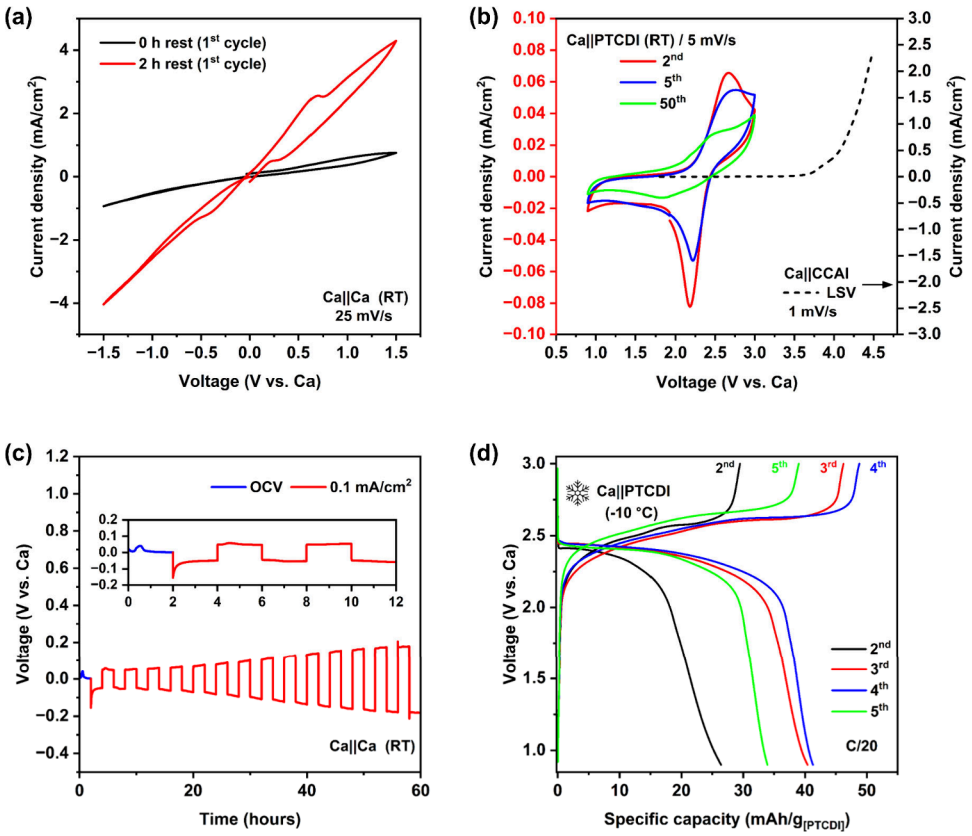

Figure 4. (a) CV of symmetric Ca||Ca coin cells at room temperature (RT). (b) CV of Ca||PTCDI and LSV of carbon coated Al (CCAl) current collector. (c) GC of symmetric Ca||Ca cells at 0.1 mA/cm^2 and 0.2 mAh/cm^2 at RT. (d) Selected charge−discharge cycles of Ca||PTCDI full cells at −10 °C.

species and to CaF_2, respectively.[14,17] Both features are consistent with interphase growth driven by Ca/precursor interfacial redox chemistry.

To explore the prospects of constructing CMBs with these electrolytes, we assessed their performance in symmetric Ca||Ca and full Ca||PTCDI coin cells, with a focus on how OCV rest periods prior to cycling influences cell behavior. Consistent with the half-cell results, the CV of Ca||Ca cells using the *in situ*−formed electrolyte displayed characteristic features associated with Ca plating/stripping (Figure 4a; Figure S8−S10), in line with previous reports.[22,23] Notably, introducing a 2 h OCV rest period markedly increased the current density, suggesting more effective interfacial conditioning of the electrodes, which is reflected in the galvanostatic Ca||Ca cycling at 0.1 mA/cm^2 and 0.2 mAh/cm^2, which proceeds with low polarization and reaches an initial overpotential of ca. 0.05 V (Figure 4c) —among the lowest reported to date for Ca metal cycling. However, after ∼60 h of cycling, the overpotential has close to doubled, pointing to a progressive buildup of a resistive interphase. As the interphase formation is highly sensitive to conditioning, we foresee possibilities to optimize it by adjusting the precursor solution formulation, for example, by altering concentrations or introducing additives such as iodine.[11,17] Moreover, the rate capability (Figure S11) is comparable to that of a CaI_2-based electrolyte, but with noticeably lower polarization.[11] Having established reversible Ca plating/stripping in half- and symmetric-cell configurations, we turn to Ca||PTCDI full cells. We start by assessing the anodic stability of the carbon-coated Al (CCAl) current collector by linear sweep voltammetry (LSV) using Ca||CCAI cells which shows minimal oxidative current up to ∼3.5 V (Figure 4b). With this adequate anodic stability of CCAl we progress to Ca||PTCDI full cells. The CV displays characteristic features in the 1.5−3.0 V range, suggesting reversible Ca^{2+}−PTCDI redox chemistry. The electrochemical response remains qualitatively similar over the initial cycles (2nd-5th), but diminishes upon extended cycling (50th cycle), due to loss of active PTCDI by dissolution into the electrolyte, a well-known challenge for organic cathode active materials.[13,24] Moving to low-temperature (−10 °C) operation may suppress the PTCDI dissolution and thus improve cycling stability, as some of us have reported upon elsewhere.[13] Here the Ca||PTCDI full cell exhibited stable cycling at a C/20 rate at −10 °C (Figure 4d) and the corresponding voltage profiles closely resemble those reported by Hou et al.[11] (Figure S12).

Furthermore, using the precursor solution with Li, Mg, and Al metal anodes suggest that the here demonstrated reversible electrochemistry can be generalized (Figure S13). In addition, it was also found to operate effectively using THF as solvent, resulting in similar Ca plating/stripping profiles (Figure S14), and likewise with an alternative amine in place of MOEA (Figure S7b).

In conclusion, we present a calcium−metal-driven electrolyte design strategy that enables stable calcium plating/stripping. Here Ca metal functions both as the negative electrode and as the sole source of Ca^{2+}, making an *in situ* generated electrolyte, thereby eliminating the need for any costly synthesis of moisture-sensitive Ca-salts. The interfacial redox chemistry between Ca and a borate−amine precursor

https://doi.org/10.1021/acsmaterialslett.6c00259
ACS Materials Lett. 2026, 8, 1761−1767

solution produces both a relatively stable CaF_2/borate-based interphase and Ca-containing solution species, including Ca^{2+}–Borate and Ca^{2+}–MOEA complexes (i.e., creating an electrolyte), which together enable reversible Ca electrochemistry. More broadly, this work highlights the promise of interphase-reaction-driven electrolyte engineering and motivates further systematic exploration of the borate–amine chemistry, which could unlock new possibilities for multivalent metal anodes, with direct implications for the advancement of CMBs and beyond.

■ ASSOCIATED CONTENT

Supporting Information

The Supporting Information is available free of charge at https://pubs.acs.org/doi/10.1021/acsmaterialslett.6c00259.

Detailed Materials and Methods (including precursor design rationale); electrochemical procedures and protocols; and additional electrochemical, SEM/EDX, FTIR, XPS, and DFT data/analyses (PDF)

■ AUTHOR INFORMATION

Corresponding Author

Zaher Slim – *Department of Physics, Chalmers University of Technology, 412 96 Göteborg, Sweden;* orcid.org/0000-0002-6437-0858; Email: zahers@chalmers.se

Authors

Hanna Andersson – *Department of Physics, Chalmers University of Technology, 412 96 Göteborg, Sweden*

Patrik Johansson – *Department of Physics, Chalmers University of Technology, 412 96 Göteborg, Sweden; ALISTORE-European Research Institute, Amiens 80039, France; Department of Chemistry – Ångström, Uppsala University, 751 21 Uppsala, Sweden;* orcid.org/0000-0002-9907-117X

Complete contact information is available at: https://pubs.acs.org/10.1021/acsmaterialslett.6c00259

Author Contributions

Z.S. conceived the idea, designed the study, conducted the experiments and DFT calculations, analyzed and interpreted the results, performed visualization (figures and schematics), wrote the first draft and led manuscript revisions. H.A. carried out supporting electrochemical and FTIR measurements and assisted with corresponding data analysis. P.J. provided mentoring to Z.S., secured funding, managed the project, and edited the manuscript. All authors reviewed the manuscript and approved the final version.

Notes

The authors declare no competing financial interest.

■ ACKNOWLEDGMENTS

Z.S. is grateful to Dr. Ezio Zanghellini for technical assistance and helpful discussions. Z.S also thanks Dr. Eric Pui Lam Tam for carrying out the XPS measurements and assisting with XPS data analysis. Special thanks to Dr. Tomooki Hosaka, Dr. Clément Pechberty, Dr. Josef Rizell and Dr. Patricia Huijbers for valuable feedback. Z.S. also thanks Dr. Kuray Dericiler and Prof. Yu Cao for assistance with EDX mapping and AES-SEM imaging, respectively. The authors acknowledge the Department of Industrial and Materials Science (IMS) and Chalmers Materials Analysis Laboratory (CMAL) for access to instrumentation and technical support. The authors thank Prof. Zoran Mandić (University of Zagreb) and Prof. Vladimir Panić (University of Belgrade) for their contributions to funding acquisition and project administration for the NATO Science for Peace and Security (SPS) programme under project number G5910, whereby the main part of the work was funded, and the additional funding from Swedish Research Council's Distinguished Professor, grant #2021-00613, on Next Generation Batteries to PJ. Z.S. acknowledges the use of OpenAI's ChatGPT for manuscript editing.

■ REFERENCES

(1) Arroyo-de Dompablo, M. E.; Ponrouch, A.; Johansson, P.; Palacín, M. R. Achievements, Challenges, and Prospects of Calcium Batteries. *Chem. Rev.* **2020**, *120*, 6331–6357.

(2) Engmann, E. T.; Yuan, Y.; Diaz, L. A.; Dai, S.; Baltrus, J. P.; Atifi, A. Efficient Room Temperature Neodymium Electrodeposition in a Calcium-Based Electrolyte. *ACS Appl. Eng. Mater.* **2023**, *1*, 2295–2303.

(3) Fu, X.; Niemann, V. A.; Zhou, Y.; Li, S.; Zhang, K.; Pedersen, J. B.; Saccoccio, M.; Andersen, S. Z.; Enemark-Rasmussen, K.; Benedek, P.; et al. Calcium-Mediated Nitrogen Reduction for Electrochemical Ammonia Synthesis. *Nat. Mater.* **2024**, *23*, 101–107.

(4) Ponrouch, A.; Frontera, C.; Bardé, F.; Palacín, M. R. Towards a Calcium-Based Rechargeable Battery. *Nat. Mater.* **2016**, *15*, 169–172.

(5) Wang, D.; Gao, X.; Chen, Y.; Jin, L.; Kuss, C.; Bruce, P. G. Plating and Stripping Calcium in an Organic Electrolyte. *Nat. Mater.* **2018**, *17*, 16–20.

(6) Li, Z.; Fuhr, O.; Fichtner, M.; Zhao-Karger, Z. Towards Stable and Efficient Electrolytes for Room-Temperature Rechargeable Calcium Batteries. *Energy Environ. Sci.* **2019**, *12*, 3496–3501.

(7) Shyamsunder, A.; Blanc, L. E.; Assoud, A.; Nazar, L. F. Reversible Calcium Plating and Stripping at Room Temperature Using a Borate Salt. *ACS Energy Lett.* **2019**, *4*, 2271–2276.

(8) Kisu, K.; Kim, S.; Shinohara, T.; Zhao, K.; Züttel, A.; Orimo, S. Monocarborane Cluster as a Stable Fluorine-Free Calcium Battery Electrolyte. *Sci. Rep.* **2021**, *11*, 7563.

(9) Leon, N. J.; Xie, X.; Yang, M.; Driscoll, D. M.; Connell, J. G.; Kim, S.; Seguin, T.; Vaughey, J. T.; Balasubramanian, M.; Persson, K. A.; Liao, C. Room-Temperature Calcium Plating and Stripping Using a Perfluoroalkoxyaluminate Anion Electrolyte. *J. Phys. Chem. C* **2022**, *126*, 13579–13584.

(10) Pavčnik, T.; Forero-Saboya, J. D.; Ponrouch, A.; Robba, A.; Dominko, R.; Bitenc, J. A Novel Calcium Fluorinated Alkoxyaluminate Salt as a next Step towards Ca Metal Anode Rechargeable Batteries. *J. Mater. Chem. A* **2023**, *11*, 14738–14747.

(11) Hou, Z.; Zhou, R.; Liu, K.; Zhu, J.; Zhang, B. A. CaI_2 -Based Electrolyte Enabled by Borate Ester Anion Receptors for Reversible Ca–Organic and Ca–Se Batteries. *Angew. Chem., Int. Ed.* **2025**, *64*, e202413416.

(12) Leon, N. J.; Ilic, S.; Xie, X.; Jeong, H.; Yang, Z.; Wang, B.; Spotte-Smith, E. W. C.; Stern, C.; Hahn, N.; Zavadil, K.; Cheng, L.; Persson, K. A.; Connell, J. G.; Liao, C. Design Principles and Routes for Calcium Alkoxyaluminate Electrolytes. *J. Phys. Chem. Lett.* **2024**, *15*, 5096–5102.

(13) Slim, Z.; Cruz-Cardona, C.; Pechberty, C.; Hosaka, T.; Mandić, Z.; Panic, V.; Johansson, P. Solvent-Mediated Electrolyte Design for Calcium Metal Batteries. *ACS Mater. Lett.* **2025**, *7*, 3235–3242.

(14) Forero-Saboya, J.; Davoisne, C.; Dedryvère, R.; Yousef, I.; Canepa, P.; Ponrouch, A. Understanding the Nature of the Passivation Layer Enabling Reversible Calcium Plating. *Energy Environ. Sci.* **2020**, *13*, 3423–3431.

(15) Forero-Saboya, J.; Bodin, C.; Ponrouch, A. A Boron-Based Electrolyte Additive for Calcium Electrodeposition. *Electrochem. Commun.* **2021**, *124*, No. 106936.

(16) Bodin, C.; Forero Saboya, J.; Jankowski, P.; Radan, K.; Foix, D.; Courrèges, C.; Yousef, I.; Dedryvère, R.; Davoisne, C.; Lozinšek, M.; Ponrouch, A. Boron-Based Functional Additives Enable Solid Electrolyte Interphase Engineering in Calcium Metal Battery. *Batter. Supercaps* **2023**, *6*, No. e202200433.
(17) Song, X.; Sun, J.; Ren, W.; Wang, L.; Yang, B.; Ning, H.; Zhang, P.; Caixiang, Z.; Tie, Z.; Zhang, X.; NuLi, Y.; Jin, Z. Iodine Boosted Fluoro-Organic Borate Electrolytes Enabling Fluent Ion-Conductive Solid Electrolyte Interphase for High-Performance Magnesium Metal Batteries. *Angew. Chem., Int. Ed.* **2025**, *64*, No. e202417450.
(18) Hou, S.; Ji, X.; Gaskell, K.; Wang, P.; Wang, L.; Xu, J.; Sun, R.; Borodin, O.; Wang, C. Solvation Sheath Reorganization Enables Divalent Metal Batteries with Fast Interfacial Charge Transfer Kinetics. *Science* **2021**, *374*, 172−178.
(19) Ren, W.; Wu, D.; NuLi, Y.; Zhang, D.; Yang, Y.; Wang, Y.; Yang, J.; Wang, J. An Efficient Bulky $Mg[B(Otfe)_4]_2$ Electrolyte and Its Derivatively General Design Strategy for Rechargeable Magnesium Batteries. *ACS Energy Lett.* **2021**, *6*, 3212−3220.
(20) Cheng, M.; Ren, W.; Zhang, D.; Zhang, S.; Yang, Y.; Lv, X.; Yang, J.; Wang, J.; NuLi, Y. Efficient Single-Perfluorinated Borate-Based Electrolytes for Rechargeable Magnesium Batteries. *Energy Storage Mater.* **2022**, *51*, 764−776.
(21) Li, Y.; Hosaka, T.; Maibach, J.; Johansson, P. Stable Anode Interphase Enabled Use of Protic Electrolytes in Sodium Metal Batteries. *Energy Storage Mater.* **2025**, *82*, 104566.
(22) Melemed, A. M.; Gallant, B. M. Electrochemical Signatures of Interface-Dominated Behavior in the Testing of Calcium Foil Anodes. *J. Electrochem. Soc.* **2020**, *167*, No. 140543.
(23) Lin, H.; Meng, J.; Guo, W.; Li, R.; Yi, Y.; Ma, Y.; Cheung, C. F.; Aurbach, D.; Xu, Z.-L. Deciphering the Dynamic Interfacial Chemistry of Calcium Metal Anodes. *Energy Environ. Sci.* **2024**, *17*, 6548−6558.
(24) Hou, Z.; Zhou, R.; Yao, Y.; Min, Z.; Lu, Z.; Zhu, Y.; Tarascon, J.; Zhang, B. Correlation between Electrolyte Chemistry and Solid Electrolyte Interphase for Reversible Ca Metal Anodes. *Angew. Chem.* **2022**, *134*, No. e202214796.

https://doi.org/10.1021/acsmaterialslett.6c00259
ACS Materials Lett. 2026, 8, 1761−1767